RESEARCH ARTICLE

In vitro model of the glial scar

Ao Fang[1,2], Zhiyan Hao[1,2], Ling Wang[1,2], Dichen Li[1,2]*, Jiankang He[1,2], Lin Gao[1,2], Xinggang Mao[3], Rubén Paz[4]

[1]School of Mechanical Engineering, Xi'an Jiaotong University, Xi'an, ShaanXi 710054, China
[2]State Key Laboratory for Manufacturing System Engineering, School of Mechanical Engineering, Xi'an Jiaotong University, Xi'an, ShaanXi 710054, China
[3]Department of Neurosurgery, Xijing Hospital, Fourth Military Medical University, Xi'an, Shaanxi Province 710032, China
[4]Departamento de Ingeniería Mecánica, Universidad de Las Palmas de Gran Canaria, 35017 Las Palmas de Gran Canaria, Spain

Abstract: The trauma of central nervous system (CNS) can lead to glial scar, and it can limit the regeneration of neurons at the injured area, which is considered to be a major factor affecting the functional recovery of patients with CNS injury. At present, the study of the glial scar model *in vitro* is still limited to two-dimensional culture, and the state of the scar *in vivo* cannot be well mimicked. Therefore, we use a collagen gel and astrocytes to construct a three-dimensional (3D) model *in vitro* to mimic natural glial scar tissue. The effects of concentration changes of astrocytes on cell morphology, proliferation, and tissue performance were investigated. After 8 days of culture *in vitro*, the results showed that the tissue model contracted, with a measured shrinkage rate of 4.5%, and the compressive elastic modulus increased to nearly 4 times. Moreover, the astrocytes of the 3D tissue model have the ability of proliferation, hyperplasia, and formation of scar clusters. It indicates that the model we constructed has the characteristics of glial scar tissue to some extent and can provide an *in vitro* model for the research of glial scar and brain diseases.

Keywords: Glial scar; *In vitro*; Three-dimensional

*Correspondence to: Dichen Li, State Key Laboratory for Manufacturing System Engineering, School of Mechanical Engineering, Xi'an Jiaotong University, Xi'an, ShaanXi 710054, China; xjtudcli@sina.com

Received: July 10, 2019; **Accepted:** July 18, 2019; **Published Online:** July 30, 2019

Citation: Fang A, Hao Z, Wang L, *et al.*, 2019, *In vitro* model of the glial scar. *Int J Bioprint*, 5(2): 235. http://dx.doi.org/10.18063/ijb.v5i2.235

1. Introduction

The central nervous system (CNS) is very complex, and trauma, disease, and infection of it is urgent problems to be solved, all of them are basically inseparable from resulting scars. Two types of scarring tissue are formed in the injured CNS. One is a fibrotic scar that is formed by fibroblasts, and the other is a glial scar, which consists of astrocytes, microglia, and other glial precursor cells[1]. Once CNS is injured, fibroblasts invade the region of the lesion and interact to form glia limitans with astrocytes[2-4]. However, fibrotic scars do not always exist in CNS tissue repair, such as no fibrotic scar formation during the astrocytic reconstruction of the blood-brain barrier[5,6]. Therefore, fibrotic scar does not play a key role in CNS tissue repair[1]. On the contrary, a glial scar plays an important role. A glial scar is mainly caused by CNS trauma. The formation of a glial scar is mainly caused by the action of astrocytes, such as barrier forming, mitosis, and migration to the injured area to fill space[7,8]. Astrocytes play a significant role in CNS injury response[9,10]. The response of them varies with the location of the injury. The ones near the damaged tissues become hypertrophic, hyperplastic, and deformed. Moreover, the glial fibrillary acidic protein (GFAP) goes up[11,12], the cells migrate[13-15], and the dense scar tissue begin to isolate the damaged area from the surrounding healthy tissue[16-18]. In general, the morphology, proliferation, and migration of astrocytes are the main causes of glial scar formation.

However, the research on the glial scar is mainly based on two-dimensional (2D) culture. Yu *et al.*[19] used a sterile plastic pipette to scratch the astrocytes in the 2D culture to simulate the damage and compared the protein content to estimate the degree of injury. In addition, they found that the surrounding part of the damaged area had also suffered a certain degree of trauma. The response to the scratching can be mimicked and this kind of 2D scratch-would model is widely used. Kimura-Kuroda *et al.*[20] constructed a glial scar-like structure by 2D coculturing of meningeal fibroblasts and brain astrocytes with transforming growth factor-β1 (TGF-β1). The model can inhibit the neurite outgrowth of neurons remarkably. In general, the traditional method of 2D cell culture cannot mimic the cell growth conditions *in vivo* and the physiological activities of normal cells. Hence, it cannot reflect the nature glial scar tissue properly. However, the three-dimensional (3D) model is expected to be able to express the glial scar effect from a more comprehensive level. Spencer *et al.*[21] constructed a kind of glial scar model that combines linear actuators to simulate axial Micro Motion around neural implants in a collagen gel. They found that local strain fields could stimulate the formation of the glial scar. Rocha *et al.*[22] built a 3D culture system mimicking the glial scar by the alginate gels embedded with astrocytes cultured in meningeal fibroblast conditioned medium. The model behaved similarly to that of the glial scar, for initiating changes in gene expression and inhibiting neuronal outgrowth. In this study, a 3D astrocytes model with collagen gel is constructed to mimic the glial scar tissue (hypertrophy and hyperplasia). The rate of gel contraction is dependent on the density of the cells within the block as well as the migration and proliferation of astrocytes.

2. Materials and Methods

In the paper, a 3D tissue was constructed using collagen gel with astrocytes, and the contraction of the tissue was examined by microscope. The immunofluorescence results of the cells were observed by laser scanning confocal microscope (LSCM). Scanning electron microscope (SEM) was used to analyze the morphology and pore size of the surface and section of the tissue. The specific process is shown in Figure 1.

2.1 Cell Isolation and Culture

Primary astrocytes were extracted from the cortices of 1-day-old mouse pups (Kunming strain, FMMU, Xi'an). The cortical tissue was removed and immersed in HBSS (Hank's balanced salt solution) (14175-095, Gibco, USA) at 4°C. The tissue was cut into pieces and digested with 0.25% trypsin (0458, Amresco, USA) for 20 min at 37°C and was transferred to complete

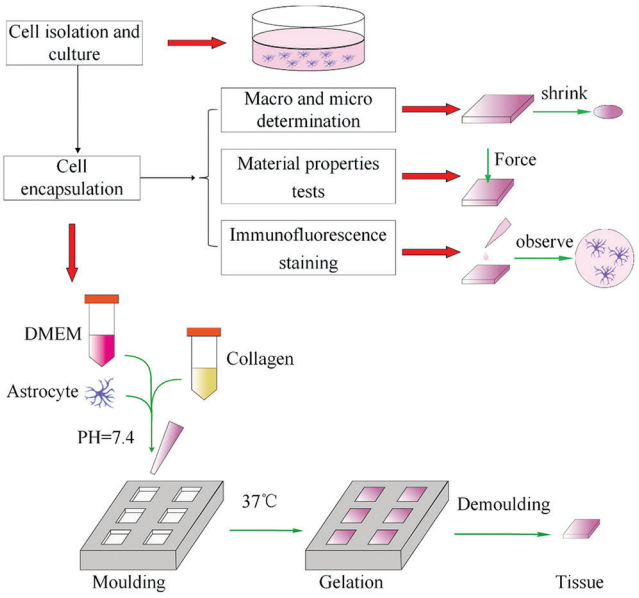

Figure 1. The flow chart of the experiment.

Dulbecco's modified eagle medium (DMEM) media containing DMEM (SH30022.01, HyClone, USA), 20% fetal bovine serum (FBS), 10270-106, Gibco), and 1% penicillin/streptomycin (P1400-100, Solarbio, USA). Finally, the medium was filtered through a 40-μm cell strainer (352340, Falcon) to dissociate the astrocytes. The isolated astrocytes were re-suspended in complete DMEM media containing 20% FBS (10270-106, Gibco) and 1% penicillin/streptomycin (P1400-100, Solarbio) at 37°C with 5% CO_2. The medium was changed every 2 days, and the cells at passage three were used for the experiment.

2.2 Cell Encapsulation

A rat tail-derived type I collagen solution (4 mg/mL in 0.1 M glacial acetic acid) was mixed with complete DMEM media at a ratio of 1:3. The pH value of the collagen and medium solution was adjusted to 7.4 before it was used to resuspend the cells at the specified concentration at 4°C. The mixture of collagen solution and astrocytes (5×10^5 cells/mL, 1×10^6 cells/mL, and 2×10^6 cells/mL) was molded into $10 \times 10 \times 2$ mm^3 block for SEM study, macroscopic determination and immunofluorescence staining. The mixture was also molded into $6 \times 6 \times 6$ mm^3 block for material properties tests. The samples were kept at 37°C for 40 min to cure. The embedding process is shown in Figure 1. Then, the tissue blocks with cells were cultured in complete DMEM media at 37°C with 5% CO_2. The collagen gels embedded in 5×10^5 cells/mL, 1×10^6 cells/mL, and 2×10^6 cells/mL were marked Group 0.5, Group 1, and Group 2, respectively.

2.3 Macroscopic and Microcosmic Determination Collagen Gels

The collagen gel blocks of 10 × 10 × 2 mm^3 were observed under the inverted fluorescence microscope (Ti-S, CHANSN, China) for macroscopic determination. The inverted fluorescence microscope software NIS was used for measuring the side lengths of the block. The side of 10 × 10 mm^2 was the measured object. The area of this face was calculated.

SEM was used for microcosmic determination. The 10 × 10 × 2 mm^3 and 6 × 6 × 6 mm^3 collagen gel blocks were both fixed with 4% paraformaldehyde for an hour. The 10 × 10 × 2 mm^3 blocks were freeze-dried by freeze dryer (VFD2000, BIOCOOL, China) overnight directly. The 6 × 6 × 6 mm^3 blocks were sliced with a freezing microtome (CM1860, Leica, German) for section views before freeze-drying. Each slice was 40 μm. After metal spraying, the freeze-dried tissues were examined using SEM (su-8010, Hitachi, Japan).

2.4 Material Mechanical Properties Tests

The 6 × 6 × 6 mm^3 collagen gel blocks were used for the determination of the compression elastic modulus in a microcomputer-controlled universal testing machine (ETM103A, Shenzhen Wance Testing Equipment Company limited, China). Before measuring, the gel blocks were fixed with 4% paraformaldehyde for an hour. And then, each of them was placed on the platform of the microcomputer-controlled universal testing machine, and the liquid on the surface of the block was removed by a plastic pipette. The loading speed was set to 2 mm/min and the compression stroke was set to 1 mm. Three samples were tested for each group.

2.5 Immunofluorescence Staining

The embedded astrocytes were fixed with 4% paraformaldehyde for an hour and washed with 1× PBS (phosphate-buffered saline, HyClone, SH30256.01) 6 times at 10 min intervals. Then, the method of freezing slice was used to obtain 40 μm thickness slices for the immunofluorescence staining of the embedded cells. Afterward, the slices were incubated in 1× PBS with 5% goat serum (AR0009, Boster, USA), 1:200 diluted primary antibody GFAP (3670S, CST, USA) and 0.3% Triton X-100 (T8200, Solarbio) overnight at 4°C. The tissues were then washed with 1× PBS 6 times at 10 min intervals. Next, the tissue was incubated in 1× PBS with 5% goat serum, 1:200 diluted secondary antibody goat anti-mouse IgG, FITC-conjugated (CW0113S, CWBIO, China), and 0.3% Triton X-100 for 4 h. Subsequently, 4,6-diamino-2-phenyl indole (DAPI) (AR1176, Boster) was added for an additional 10 min. Finally, the tissues were washed 6 times in 1× PBS at 10 min intervals and observed under a LSCM.

3. Results

3.1 Morphology and Proliferation of Astrocytes Embedded in Collagen Gel

After 8 days of cultivation, the astrocytes were distributed throughout the collagen gels and demonstrated typical stellate morphologies, and widespread process extension was observed. The process extension of the astrocytes became longer (Figure 2). To measure the proliferation, the cells were observed by laser confocal microscopy in 3D space style. DAPI was used to stain the nuclei and the concentration was obtained by dividing the number of DAPI (cells) by the volume of the 3D space. According to the results, the number of cells in the three groups increased with the increase of culture time (Figure 3). In the first 4 days, the number of cells in Group 0.5 was always lower than in Groups 1 and 2, and the concentration was below 1.5 × 10^6 cells/mL. The astrocyte process extension was also poorer compared to the other groups (Figure 2). On day 8, the cell concentration increased to 1.9 × 10^6 cells/mL, and then the cells were able to communicate and extend more easily. Compared with it,

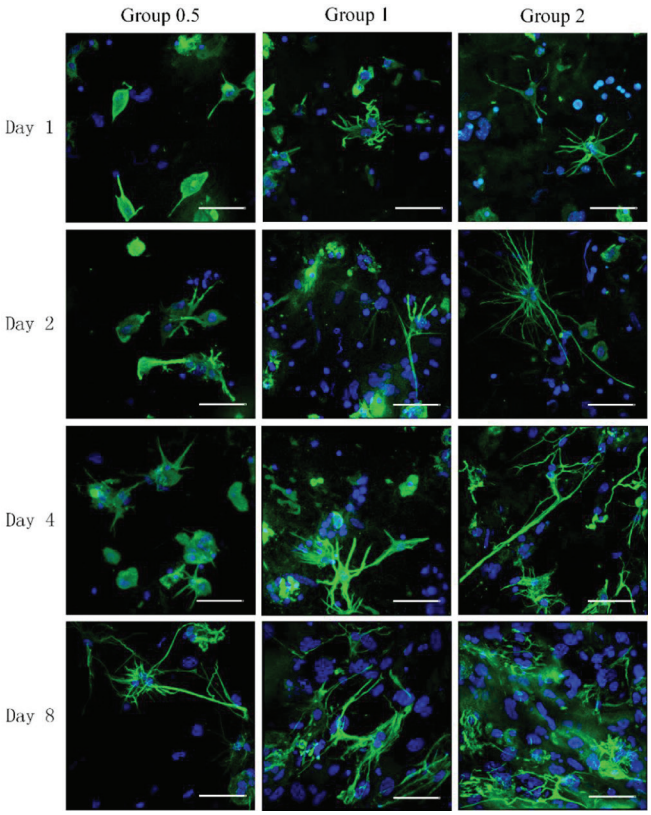

Figure 2. Immunofluorescence staining of different gradient concentration astrocytes embedded in collagen gel on day 1, day 2, day 4, and day 8. The astrocytes stained with glial fibrillary acidic protein (green) and nuclei stained with DAPI (blue). Scale bar: 50 μm.

the cell densities of Group 1 and Group 2 were larger, so did the number of the cells. In particular, the length of the protrusion extension was higher, and the cell proliferation was faster in Group 2. In addition, the further longer protrusions of the cells occurred in Group 1 and Group 2 on day 4. At the same time, the proliferation did not stop, and the cell concentration was 4.5×10^6 cells/mL for Group 2 and 3×10^6 cells/mL for Group 1. On day 8, the cell density increased further, and the cell concentration was 7.4×10^6 cells/mL for Group 2 and 4.7×10^6 cells/mL for Group 1. Especially in Group 2, the cells were still in a discrete state in some regions, with a high degree of process extension. However, the cells aggregated in many areas of Group 2. The number of cell nuclei stained with DAPI increased obviously, and a large number of cells clustered together and became denser.

3.2 The Deformation (shrinkage) of Tissue Blocks

The size of the collagen gel block was $10 \times 10 \times 2$ mm^3 and the side of 10×10 mm^2 was selected as the observation object. The vertical direction along the gel tissue was the observation direction. The area of the collagen gel blocks without cells did not change, but the embedded astrocytes ones shrank. The degree of shrinking depends on cell concentration and the days of culture (Figure 4). The area of collagen gel of Group 0.5, Group 1, and Group 2 continued to shrink with the increase of culture time, and the degree of contraction was positively correlated with the concentration of embedded cells and culture time.

The transparency of the gels also changed during the process of shrinking. As the astrocytes proliferated and migrated, the water was squeezed out, and the area was reduced continuously. When the collagen gel had just been constructed, the gel was almost transparent, but it gradually became opaque (Figure 4A). When the area of gel block shrank by 60% or more, the four corners of the block began to disappear and changed to an ellipsoid or sphere gradually. From the front view of the collagen gel block, the block was thickened in the vertical direction and the middle part of it became more and more abrupt. As the concentration of the embedded cells and the culture day increased, the lateral direction of the model was gradually shortened, the vertical direction was gradually increased, and the central portion was arched. With the process of culture, the original rectangular section became ellipsoid and gradually approximated to spherical shape at the end of the culture. On day 8, the shape of the collagen gel blocks of Group 0.5, Group 1, and Group 2 had been changed into ellipsoids or spheres and the areas of them were about 8.9%, 6.3%, and 4.5% of their initial areas, respectively (Figure 4B).

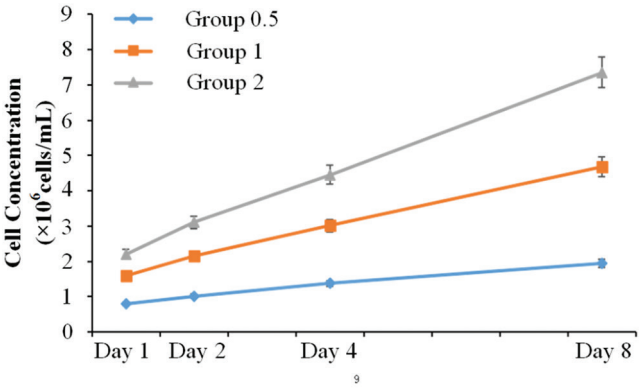

Figure 3. Proliferation of astrocytes of different concentration astrocytes embedded in collagen gel, n=4.

3.3 Effects of Astrocytes on Collagen Gel Blocks Surface

SEM tests of the surface of the samples on day 4 were carried out to analyze the reason of collagen shrinkage. The SEM images of collagen gel blocks surface showed that the embedded astrocytes and no cells blocks were

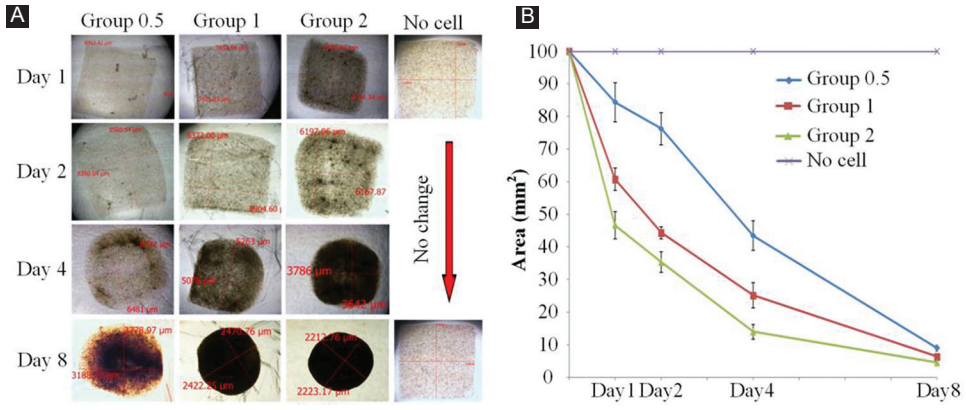

Figure 4. (**A**) The collagen gel blocks with different concentration astrocytes under the microscope. (**B**) The area of collagen gels changes with different concentration astrocytes, n=5.

quite different. The surface morphology of collagen gel blocks without cells was fibrous, porous, and flat (Figure 5C). On the contrary, the one with embedded cells had obvious folds (Figure 5D). The macroscopic gel blocks corresponding to the two kinds of surfaces are shown in Figure 5A and B. From the enlarged images, it could be found that the surface morphology of the collagen gel blocks without cells was porous (Figure 5E), and the surface morphology of the astrocytes embedded ones was almost non-porous, smooth and solid, and relatively (Figure 5F).

3.4 Effects of Astrocytes on Collagen Gel Blocks Cross Section

The cross-sectional morphology of collagen gel blocks of Group 0.5, Group 1, and Group 2 was examined by SEM (Figure 6). After the embedded astrocytes were cultured for 1 day, the collagen fiber pores of the cross sections were observed. The pores of Group 0.5 (around 10 μm) were relatively larger than the ones of the other groups. On day 2, the collagen fiber pores shrank. Similar results were obtained after 4 days in culture; the collagen fibers were aggregated, causing the pores between the fibers to shrink further; Group 0.5 shrank to about 2 μm, Group 1 shrank to about 1 μm; and Group 2 shrank to about 0.5 μm. On day 8, the pores between collagen fibers of Group 2 were almost invisible, and the pores of the Group 0.5 and Group 1 samples could be seen, but they were small, both of them around 0.5 μm (Figure 6).

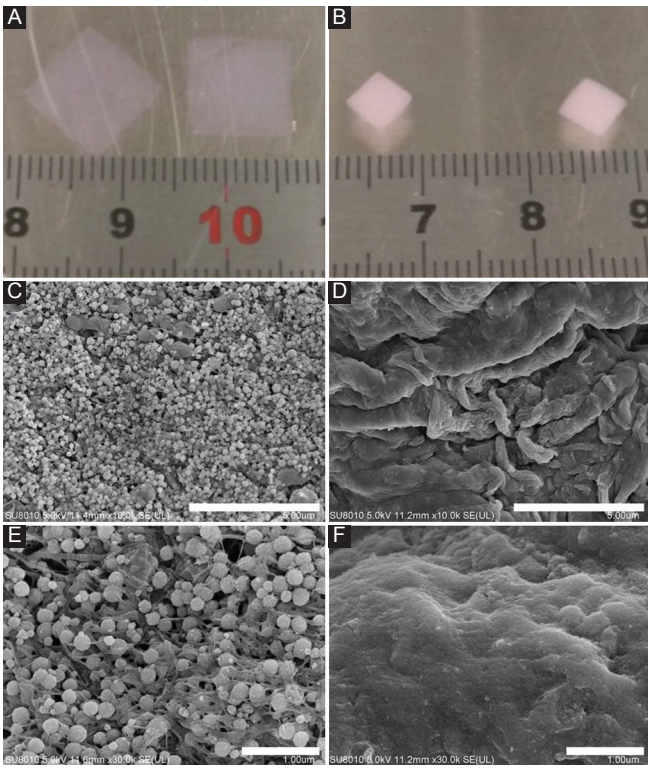

Figure 5. The surface of the collagen gel blocks on day 4. (**A**) Collagen gel block without cells. (**B**) Collagen gel blocks with astrocytes. (**C**) Scanning electron microscope (SEM) of the surface of collagen gel blocks without cells. Scale bar: 5 μm (**D**) SEM of the surface of collagen gel blocks with astrocytes. Scale bar: 5 μm. (**E**) Enlargement SEM of the surface of collagen gel blocks without cells. Scale bar: 1 μm. (**F**) Enlargement SEM of the surface of collagen gel blocks with astrocytes. Scale bar: 1 μm.

3.5 Compressive Elastic Modulus of Gel Blocks

The modulus of the glial tissue increased with the increment of culture time. Moerover, the modulus of Group 2 tissue was larger than the other two groups. In the first 2 days, Group 0.5 and Group 1 collagen tissue modulus was close. On day 4, the modulus gap widened between the two groups. On day 8, the modulus of Group 0.5 and Group 1 returned to a relatively closed state (Figure 7A). On the other hand, the modulus increased, with the increase of shrinkage rate. Overall, the Group2 modulus varied most greatly with the shrinkage. Therefore, it can be observed that for the same shrinkage change, the greater the concentration of the cells, the higher the increase of the modulus (Figure 7B).

4. Discussion

At present, the *in vitro* scar research model is limited to 2D models, and 2D culture does not characterize the culture environment *in vivo* well. In this paper, a 3D glial scar model of CNS *in vitro* was constructed using three different concentration astrocytes, and the changes of the cells and gel structure have been studied. The model can reflect the formation of glial scars from two aspects, cell and the macroscopic and microscopic perspectives of the model. From the cellular point of view, the cells proliferated and migrated. The study of proliferation and migration characteristics was carried out by adjusting the initial concentration of the cells embedded in collagen gel. We found that the higher the initial concentration and the more proliferation ability and interaction of the cells, the better for glial scar-like cluster formation. Figure 8A shows this cluster formation, which is similar to the results of literature[20]. In this reference, the authors carried out the coculture of meningeal fibroblasts and cerebral astrocytes with TGF-β1 to form a scar-like structure. The model constructed in this paper reproduces the characteristics of glial scar clusters in 3D space (Figure 8B), which has advantages compared with 2D cell growth[23,24]. In addition, the morphology of the cells embedded in collagen gel block at the concentration of 2×10^6 cells/mL is hypertrophic, hyperplastic, and deformed (Figure 9), and the similar phenomenon occurs during the glial scar formation. That is to say, the model constructed by us has similar characteristics to the glial scar in terms of

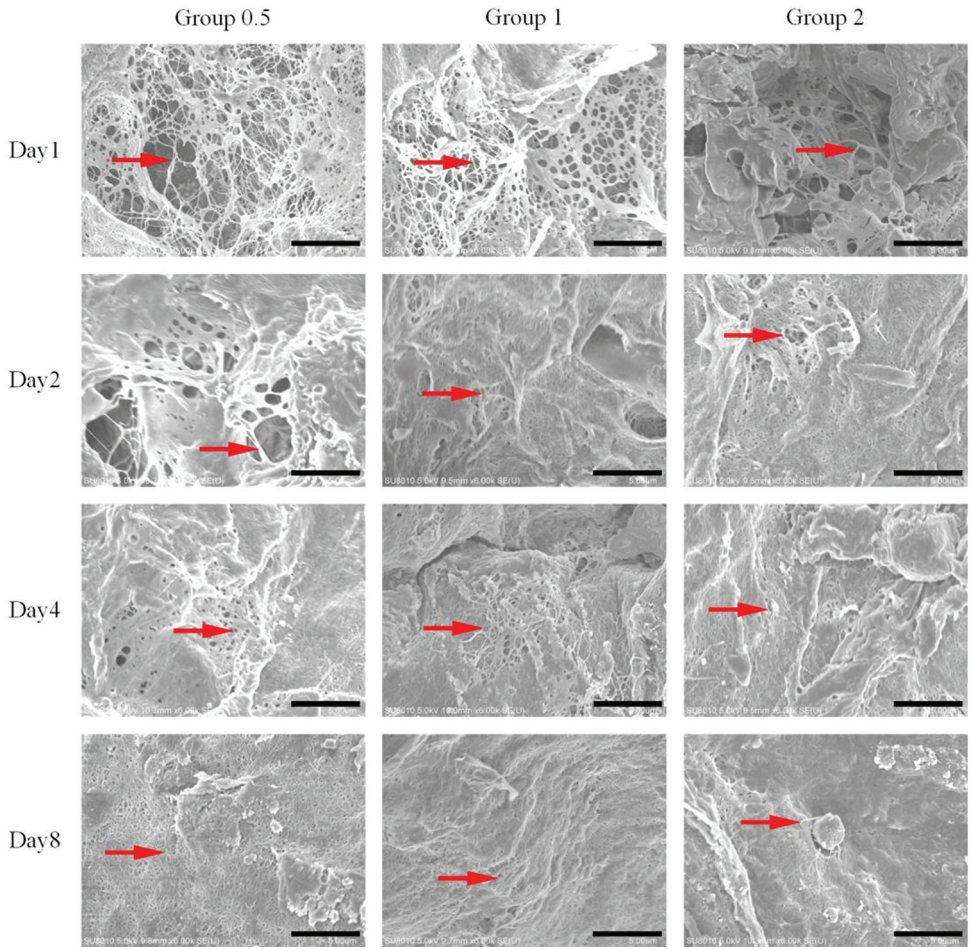

Figure 6. Scanning electron microscope images of cross sections of collagen gel blocks embedded in different concentration gradient cells. Arrows indicate the collagen fiber. Scale bar: 5 μm.

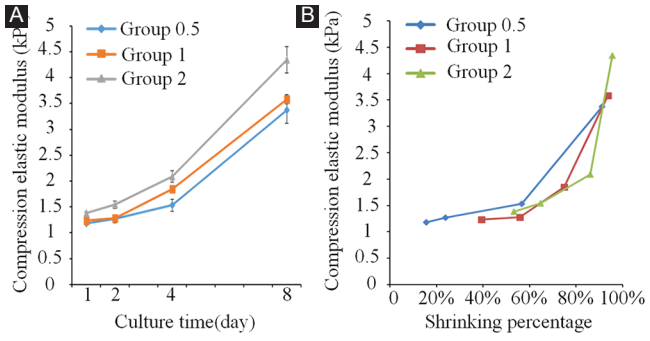

Figure 7. (**A**) Compression elastic modulus of the collagen gel blocks changes with the increase of culture time. (**B**) Compression elastic modulus of the collagen gel blocks changes with the shrink of the blocks.

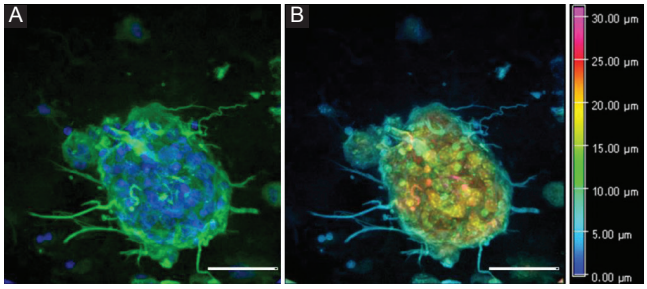

Figure 8. (**A**) Glial scar-like cluster formed by astrocytes aggregation in three-dimensional collagen gel tissue, cells stained with glial fibrillary acidic protein (green) for astrocytes, DAPI (blue) for nuclei. (**B**) Images (depth decoding) of glial scar-like cluster. Different colors represent the different planes along the Z-axis, Scale bars: 50 μm.

cell morphology[19], which further proves that the tissue model has the potential to form glial scars.

From the macroscopic and microscopic point of view, the collagen gel block with astrocytes shrinks with the increase of culture time. However, the size of the collagen gel block without cells does not change significantly, the reason why the shrinkage of collagen gel is mainly related to the proliferation and migration of astrocytes, which are similar to the glial scar formation in the CNS *in vivo*[12,18]. In addition, the gel shrinking in culture is similar to the phenomenon of fibroblast collagen gel tissue[25], which is related to the formation of scars, wound repair,

and filling. Thus, the proposed 3D collagen gel tissue constructed with astrocytes has scar formation properties, and the glial scars are mainly produced by astrocytes. It is quite coincidental that the similar phenomenon of tissue shrinking also occurs in the brain of a Sorex araneus. Scientists have discovered that the skull of the Sorex araneus pup shrinks in the late summer, as well as the brain, whose weight is also reduced. During the winter, the part of brain lost can grow back partly. This phenomenon is called Dehnel's phenomenon[26-28]. It is similar to the results of this article, occurring in the brain. To a certain extent, it may provide some reference for the study of brain plasticity and evolution. It may have a certain value for reference to the study of brain plasticity and evolution.

On the basis of this shrinkage, the folds can be found on the surface of the block, and the pores are reduced with the increase of culture time. Tallinen *et al*.[29] used a similar principle to construct a fold model of the human brain from a macro perspective. At this stage, the cells traction caused the deformation of the extracellular matrix[30-32], resulting in a stronger collagen fiber aggregation. With different initial cell concentrations, the degree of reduction is also different. The higher the concentration, the more cells proliferate and migrate, and the more seriously the gel tissue shrinks. The collagen gel with astrocytes shrinks due to cell proliferation and migration. Consequently, the collagen fibers gradually extrude each other, the surface pores disappear, and the fiber pores decrease. Meanwhile, the surface of the collagen gel is deformed to form a relatively solid and wrinkled surface because of the movement of the cells. The process of gel contraction is similar to the course of wound healing[33]. The force produced by cell proliferation and migration does not affect the collagen gel without cells. Hence, the surface remains flat and porous. In addition, the shrinkage rates of blocks with different concentration astrocytes were relatively similar on day 8, but the moduli of them were quite different. This indicates that the concentration of cells also has a certain effect on the modulus when the collagen gel shrinks. The higher the cell concentration, the larger the collagen tissue modulus. From this, the reason for collagen gel macroscopic and microscopic size-changing can be inferred (Figure 10). The results of the experiment can demonstrate that the model we constructed can form glial scars.

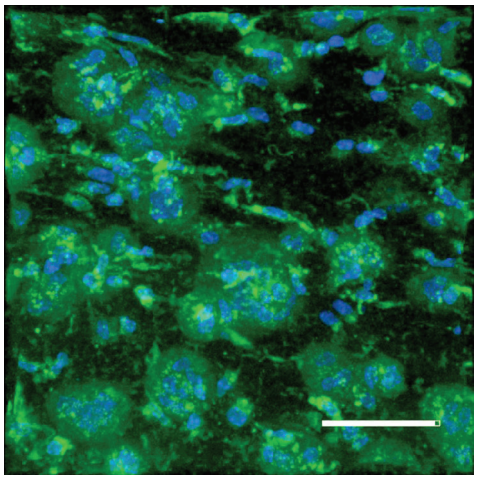

Figure 9. The hypertrophic cytoplasm of astrocytes embedded in collagen gel on day 8, astrocytes were stained by glial fibrillary acidic protein in green, nuclei were stained by DAPI in blue, Scale bars: 50 μm.

5. Conclusion

In this study, a 3D astrocytes model with collagen gel *in vitro* has been constructed. This model shows the characteristics of the glial scar (hypertrophy and hyperplasia). The constructed 3D model reveals overall shrinkage with the prolongation of culture time. On the other hand, the shrinkage rate and compression elastic

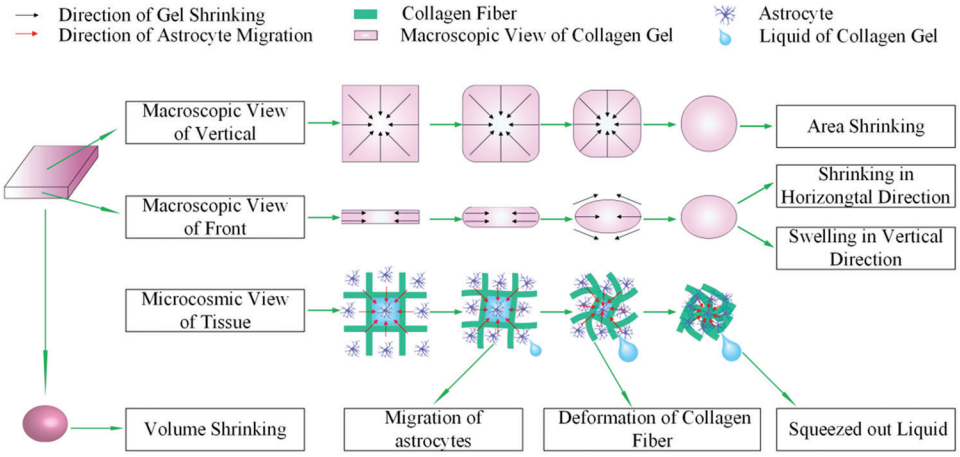

Figure 10. The reason for collagen gel block size changing from macroscopic and microscopic.

modulus are positively correlated with the culture time and cell concentration, because of the migration and proliferation of astrocytes. The construction method of the 3D tissue studied in this paper can be used to create *in vitro* glial tissue models, which can be useful for the study of glial scar and related brain diseases.

Acknowledgments

The work was supported by the Program of the National Natural Science Foundation of China [51675411] and the Youth Innovation Team of Shaanxi Universities.

Authors' Contributions

AF and LW designed the study; AF and ZY experimented. AF, LW, and RP drafted the manuscript. DC, LW, LG, XG, and JK coordinated the project and discussed the results. All authors read and approved the final manuscript.

Conflicts of Interest

The authors declare that they do not have any competing interests.

References

1. Kawano H, Kimura-Kuroda J, Komuta Y, *et al*., 2012, Role of the Lesion Scar in the Response to Damage and Repair of the Central Nervous System. *Cell Tissue Res*, 349:169-80. DOI 10.1007/s00441-012-1336-5.
2. Aand JM, Berry M, 1985, Observation on Astrocyte Response to a Cerebral Stab Wound in Adult Rats. *Brain Res*, 327:61-9.
3. Maxwell W, Follows R, Ashhurst D, *et al*., 1990, The Response of the Cerebral Hemisphere of the Rat to Injury. I. The Mature Rat. *Philos Trans R Soc Lond B Biol Sci*, 328:479-500. DOI 10.1098/rstb.1990.0121.
4. Mand CS, Fawcett J, 2001, The Astrocyte/Meningeal Cell Interface a Barrier to Successful Nerve Regeneration? *Cell Tissue Res*, 305:267-73. DOI 10.1007/s004410100384.
5. Yoshioka N, Kimura-Kuroda J, Saito T, *et al*., 2011, Small Molecule Inhibitor of Type I Transforming Growth Factor-beta Receptor Kinase Ameliorates the Inhibitory Milieu in Injured Brain and Promotes Regeneration of Nigrostriatal Dopaminergic Axons. *J Neurosci Res*, 89(3):381-93. DOI 10.1002/jnr.22552.
6. Yoshioka N, Hisanaga S, Kawano H, 2010, Suppression of Fibrotic Scar Formation Promotes Axonal Regeneration Without Disturbing Blood-Brain Barrier Repair and Withdrawal of Leukocytes After Traumatic Brain Injury. *J Comp Neurol*, 518:3867-81. DOI 10.1002/cne.22431.
7. Mand P, Nilsson M, 2005, Astrocyte Activation and Reactive Gliosis. *Glia*, 50:427-34.
8. Anderson MF, Blomstrand F, Blomstrand C, *et al*., 2003, Astrocytes and Stroke: Networking for Survival? *Neurochem Res*, 28(2):293-305. DOI 10.1023/a:1022385402197.
9. Tatsumi K, Haga S, Matsuyoshi H, *et al*., 2005, Characterization of Cells with Proliferative Activity after a Brain Injury. *Neurochem Int*, 46(5):381-9. DOI 10.1016/j.neuint.2004.12.007.
10. Norenberg MD, 1994, Astrocyte Responses to CNS Injury. *J Neuropathol Exp Neurol*, 53(3):213-20.
11. Gao K, Wang CR, Jiang F, *et al*., 2013, Traumatic Scratch Injury in Astrocytes Triggers Calcium Influx to Activate the JNK/c-Jun/AP-1 Pathway and Switch on GFAP Expression. *Glia*, 61(12):2063-77. DOI 10.1002/glia.22577.
12. Sofroniew MV, 2015, Astrogliosis. *Cold Spring Harb Perspect Biol*, 7(2):a20420.
13. Kozai TDY, Jaquins-Gerstl AS, Vazquez AL, *et al*., 2015, Brain Tissue Responses to Neural Implants Impact Signal Sensitivity and Intervention Strategies. *ACS Chem Neurosci*, 6(1):48-67. DOI 10.1021/cn500256e.
14. Woeppel K, Qand Y, Cui XT, 2017, Recent Advances in Neural Electrode-Tissue Interfaces. *Curr Opin Biomed Eng*, 4:21-31.
15. Chen N, Luo B, Yang IH, *et al*., 2018, Biofunctionalized Platforms Towards Long-term Neural Interface. *Curr Opin Biomed Eng*, 6:81-91.
16. Jand S, Miller JH, 2014, Regeneration Beyond the Glial Scar. *Exp Neurol*, 253(1):197-207.
17. Rand FA, Silver J, 2016, Targeting Astrocytes in CNS Injury and Disease: A Translational Research Approach. *Prog Neurobiol*, 144:173-87.
18. Zhan JS, Gao K, Chai RC, *et al*., 2017, Astrocytes in Migration. *Neurochem Res*, 42(1):272-82.
19. Yu AC, Lee YL, Eng LF, 1993, Astrogliosis in Culture: I. The Model and the Effect of Antisense Oligonucleotides on Glial Fibrillary Acidic Protein Synthesis. *J Neurosci Res*, 34(3):295-303. DOI 10.1002/jnr.490340306.
20. Kimura-Kuroda J, Teng X, Komuta Y, *et al*., 2010, An *in vitro* Model of the Inhibition of Axon Growth in the Lesion Scar Formed after Central Nervous System Injury. *Mol Cell Neurosci*, 43(2):177-87. DOI 10.1016/j.mcn.2009.10.008.
21. Spencer KC, Sy JC, Falcón-Banchs R, *et al*., 2017, A Three Dimensional *in vitro* Glial Scar Model to Investigate the Local Strain Effects from Micromotion Around Neural Implants. *Lab A Chip*, 17(5):795-804. DOI 10.1039/c6lc01411a.
22. Rocha DN, Ferraz-Nogueira JP, Barrias CC, *et al*., 2015, Extracellular Environment Contribution to Astrogliosis Lessons Learned from a Tissue Engineered 3D Model of

the Glial Scar. *Front Cell Neurosci*, 9(1):377. DOI 10.3389/fncel.2015.00377.

23. García-Fernández L, Halstenberg S, Unger RE, *et al*., 2010, Anti-Angiogenic Activity of Heparin-like Polysulfonated Polymeric Drugs in 3D Human Cell Culture. *Biomaterials*, 31(31):7863-72. DOI 10.1016/j.biomaterials.2010.07.022.
24. Jand S, Pompe T, 2018, Biomimetic Tumor Microenvironments Based on Collagen Matrices. *Biomater Sci*, 6:2009-24. DOI 10.1039/c8bm00303c.
25. Bell E, Ivarsson B, Merrill C, 1979, Production of a Tissue-like Structure by Contraction of Collagen Lattices by Human Fibroblasts of Different Proliferative Potential *in vitro*. *Proc Natl Acad Sci U S A*, 76(3):1274-8. DOI 10.1073/pnas.76.3.1274.
26. Lázaro J, Dechmann DKN, Lapoint S, *et al*., 2017, Profound Reversible Seasonal Changes of Individual Skull Size in a Mammal. *Curr Biol*, 27(20):3576. DOI 10.1016/j.cub.2017.10.064.
27. Lapoint S, Keicher L, Wikelski M, *et al*., 2017, Growth Overshoot and Seasonal Size Changes in the Skulls of Two Weasel Species. *R Soc Open Sci*, 4(1):160947. DOI 10.1098/rsos.160947.
28. Lázaro J, Hertel M, Sherwood CC, *et al*., 2018, Profound Seasonal Changes in Brain Size and Architecture in the Common Shrew. *Brain Struct Funct*, 223:2823-40. DOI 10.1007/s00429-018-1666-5.
29. Tallinen T, Chung JY, Rousseau F, *et al*., 2016, On the Growth and form of Cortical Convolutions. *Nat Phys*, 12(6):588-93.
30. Checa S, Rausch MK, Petersen A, *et al*., 2014, The Emergence of Extracellular Matrix Mechanics and Cell Traction Forces as Important Regulators of Cellular Self-organization. *Biomech Model Mechanobiol*, 14(1):1-13. DOI 10.1007/s10237-014-0581-9.
31. Galbraith CG, Mand YK, Sheetz MP, 2002, The Relationship between Force and Focal Complex Development. *J Cell Biol*, 159(4):695-705. DOI 10.1083/jcb.200204153.
32. Riveline D, Zamir E, Balaban NQ, *et al*., 2001, Focal Contacts as Mechanosensors. Externally Applied Local Mechanical Force Induces Growth of Focal Contacts by an Mdia1-Dependent and Rock-Independent Mechanism. *J Cell Biol*, 153(6):1175-86. DOI 10.1083/jcb.153.6.1175.
33. Corin KA, Gibson LJ, 2010, Cell Contraction Forces in Scaffolds with Varying Pore Size and Cell Density. *Biomaterials*, 31(18):4835-45. DOI 10.1016/j.biomaterials.2010.01.149.